

DISCLAIMER

This report was prepared as an account of work sponsored by an agency of the United States Government. Neither the United States Government nor any agency thereof, nor any of their employees, makes any warranty, express or implied, or assumes any legal liability or responsibility for the accuracy, completeness, or usefulness of any information, apparatus, product, or process disclosed, or represents that its use would not infringe privately owned rights. Reference herein to any specific commercial product, process, or service by trade name, trademark, manufacturer, or otherwise does not necessarily constitute or imply its endorsement, recommendation, or favoring by the United States Government or any agency thereof. The views and opinions of authors expressed herein do not necessarily state or reflect those of the United States Government or any agency thereof.

MATERIALS SURFACE MODIFICATION BY PLASMA BOMBARDMENT UNDER SIMULTANEOUS EROSION AND REDEPOSITION CONDITIONS

UCLA/PPG--992

DE86 014345

Y.Hirooka, D.M.Goebel, R.W.Conn,
G.A.Campbell, W.K.Leung
K.L.Wilson*, W.Bauer*, R.A.Causey*,
D.H.Morse* and J.Bohdansky**

UCLA-PPG-992

July 1986

Department of Mechanical, Aerospace, and Nuclear Engineering,
Center for Plasma Physics and Fusion Engineering,
University of California, Los Angeles
Los Angeles, California 90024, USA

*Physics Research Division,
Sandia National Laboratories
Livermore, California 94550, USA

**Max-Planck-Intitut fur Plasmaphysik,
EURATOM-Association,
D-8046 Garching, FRG

Invited paper at Workshop on Surface Modification by Plasma-Wall Interaction
at Princeton, May 1-2, 1986 (to be published in Nucl. Instr. & Methods-B)

MASTER

DISTRIBUTION OF THIS REPORT IS UNLIMITED

DISCLAIMER

This report was prepared as an account of work sponsored by an agency of the United States Government. Neither the United States Government nor any agency thereof, nor any of their employees, makes any warranty, express or implied, or assumes any legal liability or responsibility for the accuracy, completeness, or usefulness of any information, apparatus, product, or process disclosed, or represents that its use would not infringe privately owned rights. Reference herein to any specific commercial product, process, or service by trade name, trademark, manufacturer, or otherwise, does not necessarily constitute or imply its endorsement, recommendation, or favoring by the United States Government or any agency thereof. The views and opinions of authors expressed herein do not necessarily state or reflect those of the United States Government or any agency thereof.



MECHANICAL, AEROSPACE AND
NUCLEAR ENGINEERING DEPARTMENT
SCHOOL OF ENGINEERING AND APPLIED SCIENCE
LOS ANGELES, CALIFORNIA 90024

August 5, 1986

Ms. Evelyn Bolton
U.S. Department of Energy
Technical Information Center
P.O. Box 62
Oak Ridge, TN 37831

Dear Evelyn:

Enclosed are 134 copies of UCLA-PPG-992, "Materials Surface Modification by Plasma Bombardment under Simultaneous Erosion and Redeposition Conditions." These are for distribution to the UC20c (subdivision only) list and to 78 international addresses, for which I have provided plain mailing labels.

Many thanks for your assistance in their distribution.

Sincerely,

A handwritten signature in cursive script that reads "Pat Fina".

Pat Fina

enclosures in one box

U. S. DEPARTMENT OF ENERGY

DOE F 1332.15 (10-84)
(Formerly RA-426)

DOE AND MAJOR CONTRACTOR RECOMMENDATIONS FOR
ANNOUNCEMENT AND DISTRIBUTION OF DOCUMENTS

OMB Approval
No. 1910-1400

See instructions on Reverse Side

1. DDE Report No. UCIA-PPG-992	2. DOE Contract No. DE-AT03-84EP52104	3. Distribution Category No. UC20c (subdivision only)
-----------------------------------	--	--

4. Title
Materials Surface Modification by Plasma Bombardment under Simultaneous

5. Type of Document ("x" one) Frosion and Redeposition Conditions

Scientific and technical report

Conference paper: Title of conference _____

Date of conference _____

Exact location of conference _____

Sponsoring organization _____

Other (Specify) _____

6. Copies Transmitted ("x" one or more)

Copies being transmitted for unclassified standard distribution by OSTI/TIC.

Copies being transmitted for classified documents as contained in M-3679.

Copies being transmitted for special distribution.

Two completely legible, reproducible copies being transmitted to OSTI/TIC.

Thirty copies being transmitted to OSTI/TIC for OSTI processing and NTIS sales.

7. Recommended Distribution ("x" one)

Unrestricted, unlimited distribution.

Make available only

Classified—to M-3679 addressees only.

To U. S. Government agencies and their contractors.

To DOE offices only.

To DOE and WPAS contractors.

To DOE and any DOE contractor.

Within USA only.

Other—specify in item 14 below.

Refer all requests to _____

8. Recommended Announcement ("x" one)

Unrestricted, unlimited announcement.

Limit to U. S. Govt. agencies and contractors.

Limit to DOE and WPAS contractors.

Limit to applied technology contractors.

Limit to section 148 contractors.

Limit to authorized classified sites only.

Archives only—No announcement.

9. Future Handling of Limited Reports

After _____, this report may be reprocessed as item 7, _____ and 8, _____
(Date)

10. Reason for Restriction Recommended in 7 or 8 above. (Explain fully) _____

11. Patent and Technology Transfer Information

Does this information product disclose any new equipment, process, or material? No Yes If so, identify page nos. _____

Has an invention disclosure been submitted to DOE covering any aspect of this information product? No Yes

If yes, identify the DOE disclosure number and to whom the disclosure was submitted. _____

Are there any patent-related objections to the release of this information product? No Yes If so, state these objections.

("x" one) a. DOE patent clearance has been granted by responsible DOE patent group.

b. Document has been sent to responsible DOE patent group for clearance.

12. Does this information product contain? (Check all applicable boxes)

Copyrighted material (attach release)

Proprietary information (page numbers _____)

National security information

Restricted data

Formerly restricted data

Applied technology

Section 148

Other (explain) applied plasma physics

13. Copy Reproduction and Distribution

Total number of copies reproduced _____, Number of copies distributed outside originator (exclude copies to OSTI/TIC) _____

14. Additional information or Remarks (Continue on separate sheet, if necessary)

15. Submitted by (Name and Position) (Please print or type)

Pat Fina

Organization

UCLA

Signature

Pat Fina

Phone

(213) 825-5090

Date

8/5/86

INSTRUCTIONS

Who uses this form: All DOE offices and DOE contractors except those contractors and grantees specifically instructed by their DOE contract administrator to use the shorter Form DOE F 1332.16.

When to use: Submit one copy of this form with each report title that is sent to the DOE Office of Scientific and Technical Information (OSTI) in accordance with the requirements of DOE Order 1430.1. Additional instructions concerning report preparation, etc., can be found in DOE Order 1430.2. Questions may be referred to OSTI on FTS 626-1268 or commercial 615-576-1268.

Where to send: Forward this form and the documents to:

U. S. Department of Energy
Office of Scientific and Technical Information
Technical Information Center
P. O. Box 62
Oak Ridge, TN 37831

Item instructions:

Item 1. A standard report code system has been established for numbering DOE reports. A unique number that is complete and accurate is essential. The following specific instructions apply:

(a) **DOE Program Office Reports**—Use DOE/and the two letters identifying the Assistant Secretary under whose authority the program office operates at the beginning of the report number. Complete the number with dashes and the report sequence number as obtained from the Chief of Printing Procurement (MA 234.21). Example: DOE/NE-193.

(b) **DOE Field Organization Reports**—Use DOE/and the two letters identifying the organization responsible for the report (e.g., OR for Oak Ridge; BP for Bonneville Power, etc.). Complete the number with dashes and a report sequence number as assigned by the Technical Information Officer at the site. Example: DOE/OR-759.

(c) **Major Project Office Reports**—Use DOE/and the two or three digit identifier for the organization responsible for the report (e.g., LLW for Low Level Waste, etc.). The identifiers will be assigned by OSTI. Complete the number with dashes and a report sequence number as assigned at the project office. Example: DOE/LLW-198.

(d) **Contractor Reports**—Major contractors have been assigned report codes by OSTI. Other contractors will use DOE/and the final seven characters (two letters and five digits) from the applicable contract or grant number. A slash mark must separate the letters from the digits. Complete the number with dashes followed by a sequential number for each report generated under the contract. Example for the first report generated under contract number DE-AC03-79NE01834: DOE/NE/01834-1.

Reports that are issued in multivolumes, parts, or revisions, etc., should be numbered as follows:

DOE/NE/01834-1 Vol. 1
DOE/NE/01834-1 Pt. 1
DOE/NE/01834-1 Rev. 1

Caution: Report numbers are to be structured exactly as specified in the above examples. Modifications, if essential, must be approved by OSTI.

Item 2. Insert DOE contract number under which the work was funded.

Item 3. Insert the appropriate distribution category from DOE/TIC-4500 or M-3679 for unclassified and classified documents, respectively, whether or not printed for standard distribution.

Item 4. Give title exactly as on the document itself unless title is classified. In that case, omit title and state "classified title" in the space for Item 4.

Item 5. Self-explanatory.

Item 6. a. If box a is checked, the number of copies specified for the appropriate category or categories in DOE/TIC-4500 will be forwarded to OSTI for distribution.

b. If box b is checked, the number of copies as specified in M-3679 for OSTI/TIC should be provided. If OSTI is to make standard distribution, so indicate in item 14.

c. If box c is checked, mailing labels should be provided OSTI if possible.

d. If box d is checked, at least one copy will be original ribbon or offset and be completely legible as per DOE Order 1430.2. A high-contrast xerox copy is acceptable as a second reproducible copy. Classified documents—send one copy except where distribution requires more copies.

e. If box e is checked, 30 copies will be forwarded to OSTI/TIC.

Item 7. Distribution is made by OSTI using standard distribution lists or on request. Limitations and restrictions should not be placed on the distribution of DOE funded R&D results unless the submitting site has received DOE programmatic guidance to do so.

If box a is checked for an unclassified document, it may be distributed by OSTI/TIC (after patent clearance) to addresses listed in DOE/TIC-4500 for the appropriate distribution category. The reports are also provided to the National Technical Information Service for sale to the public.

If box b is checked for classified document, it may be distributed by OSTI to addresses listed in M-3679 for the appropriate distribution category unless distributed by the originating site.

If any box other than a is checked, the recommended limitations will be followed unless OSTI receives other instructions from the responsible DOE program division.

Box h or i may be checked in order to specify special instructions, such as "Make available only as specifically approved by the program division."

Item 8. DOE is obligated to announce (printed or electronic media) the results of its federally funded R&D to the widest extent possible. Sites should not recommend announcement limitations unless they have received DOE programmatic guidance to do so. Recommended announcement limitations can be less restrictive than recommended distribution limitations.

Item 9. For limited reports, originators are strongly encouraged to specify unlimited or less-limited processing after a certain time period. Indicate the date and the less limited reprocessing categories from items 7 and 8.

Item 10. Self-explanatory.

Item 11. It is assumed that there is no objection to publication from the standpoint of the originating organization's patent interest. Otherwise explain in Item 14.

Item 12. If the proprietary information block is checked, give the page numbers if possible.

Item 13. Self-explanatory.

Item 14. Self-explanatory.

Item 15. Enter name of person to whom inquiries concerning the recommendations on this form may be addressed. Please give FTS phone number if possible.

MATERIALS SURFACE MODIFICATION BY PLASMA BOMBARDMENT
UNDER SIMULTANEOUS EROSION AND REDEPOSITION CONDITIONS

Y.Hirooka, D.M.Goebel, R.W.Conn, G.A.Campbell, and W.K.Leung

Department of Mechanical, Aerospace, and Nuclear Engineering,
Center for Plasma Physics and Fusion Engineering,
University of California, Los Angeles
Los Angeles, California 90024, USA

K.L.Wilson, W.Bauer, R.A.Causey, and D.H.Morse

Physics Research Division,
Sandia National Laboratories
Livermore, California 94550, USA

J.Bohdansky

Max-Planck-Institut für Plasmaphysik,
EURATOM-Association,
D-8046 Garching, FRG

/ BSTRACT

The first in-depth investigation of surface modification of materials by continuous, high-flux argon plasma bombardment under simultaneous erosion and redeposition conditions have been carried out for copper and 304 stainless steel using the PISCES facility. The plasma bombardment conditions are: incident ion flux range from 10^{17} to 10^{19} ions $\text{sec}^{-1}\text{cm}^{-2}$, total ion fluence is controlled between 10^{19} and 10^{22} ions cm^{-2} , electron temperature range from 5 to 15 eV, and plasma density range from 10^{11} to 10^{13} cm^{-3} . The incident ion energy is 100 eV. The sample temperature is between 300 and 700K.

Under redeposition dominated conditions, the material erosion rate due to the plasma bombardment is significantly smaller (by a factor up to 10) than that can be expected from the classical ion beam sputtering yield data. It is found that surface

morphologies of redeposited materials strongly depend on the plasma bombardment condition. The effect of impurities on surface morphology is elucidated in detail. First-order modelings are implemented to interpret the reduced erosion rate and the surface evolution. Also, fusion related surface properties of redeposited materials such as hydrogen reemission and plasma driven permeation have been characterized.

1. INTRODUCTION

Erosion of materials for plasma interactive surface components such as limiters and divertor plates can be a major source of impurities in operating plasmas in a magnetic fusion device. These impurity elements will be reionized within the plasma by electron impact, which results in an increase in Z_{eff} . However, the presence of plasma flow to the edge region leads to a redeposition of reionized impurities on surface components [1]. For long-pulse or steady-state devices, material erosion can also lead to a shortened lifetime of surface components. However, the role of redeposition is still unclear. It may reduce the net erosion rate of materials, but it will also modify the surface morphology in a yet-to-be explored manner. Furthermore, the modified surface morphology and erosion behavior of materials might be influential one another.

In our previous work [2], the first non-tokamak, controlled plasma-wall interaction study was conducted using the PISCES facility with the main objective of understanding the mechanism of simultaneous erosion and redeposition behavior of materials. It was found that redeposition of materials resulted in a reduction of the net erosion yield relative to the classical sputtering yield. Also, the preliminary scanning electron microscope observation indicated strongly modified surface morphologies by plasma bombardment. In the present work, extensive characterization of redeposited materials has been done to elucidate the impact of surface modification by plasma bombardment on a wide range of

fusion engineering. This paper presents the first results of detailed investigation of surface modification of materials by plasma bombardment under simultaneous erosion and redeposition.

2. EXPERIMENTAL PROCEDURE

The PISCES facility and material experiments were previously described in detail elsewhere [2,3,4]. Here, the experimental procedure is outlined. A schematic diagram of the target sample and movable Langmuir probe in the linearly magnetized plasma stream is shown in fig.1. A mechanically polished disk sample with a diameter of 2.5 cm was placed on a target holder. The magnetic field is 250 gauss and perpendicular to the target surface. The Langmuir probe was moved in front of the target surface to measure the electron temperature and plasma density. During the probe measurement, the sample surface was protected by a movable shutter plate. The electron temperature was typically in the range from 5 to 20 eV, and the plasma density was in the range from 10^{11} to 10^{13} cm^{-3} .

The plasma bombardment energy was set at 100 eV in this study. The ion flux was in the range from 5×10^{17} to 5×10^{18} ions $\text{sec}^{-1} \text{cm}^{-2}$. This means that the target surface is subject to a heat flux up to 80 W cm^{-2} . Consequently, the target temperature was controlled by air or water cooling, depending on the heat flux and selected temperature. The target was set at temperatures between 300 to 1000K, which can be measured by a thermocouple attached on the sample holder. The total ion fluence was varied in the range from 10^{19} to 10^{22} ions cm^{-2} . Plasma bombarded samples were weighed to evaluate the net erosion and analyzed with a variety of surface analysis techniques including SEM (Scanning Electron Microscopy), EMPA (Electron Micro Probe Analysis), AES (Auger Electron Spectroscopy), SIMS (Secondary Ion Mass Spectroscopy), NRA (Nuclear Reaction Analysis) and RBS (Rutherford Backscattering Spectroscopy).

3. GENERAL CONSIDERATIONS OF EXPERIMENTAL CONDITIONS

Of particular interest is to compare the PISCES and conventional ion beam experiments from a surface modification viewpoint. Historically, ion beam experiments often employed ion fluxes between 10^{13} and 10^{15} ions $\text{sec}^{-1} \text{cm}^{-2}$ and ion energies between 5 and 20 keV to simulate high energy ions or charge exchange neutrals escaping from the core plasma of a magnetic fusion device [5]. The ion implantation depth in this energy range is generally above a few hundred angstroms. Under these conditions, the surface modification by both blistering and sputtering was observed, depending on the selected ion-target combination [6]. In the present work utilizing the PISCES facility, the argon ion flux is typically 10^{18} ions $\text{sec}^{-1} \text{cm}^{-2}$, and the bombardment energy is 100 eV to simulate the edge-plasma flow. As shown in fig.2, the ion implantation depth is quite shallow at this energy. Also, the recession depth of the surface per unit time due to sputtering at these high ion fluxes far exceeds the ion implantation depth under typical plasma bombardment conditions (see table 1). This means that the retention of implanted ions must be small compared with that for high energy ion bombardment cases. These particular features of a high flux and low energy plasma bombardment will not meet the general blistering criteria [7]. Therefore, one may well expect that sputtering is the predominant process to control the surface modification of materials in the present study, as will be shown later.

Another important comparison should be made between the nature of redeposition in the PISCES facility and in large toroidal fusion devices such as tokamaks. Due to impurity transport in the toroidal and poloidal directions, it is not surprising to see redeposited materials via elemental interchange between different surface components exposed to the plasma in a tokamak after an extensive period of discharge experiments[8]. Redepositing particles are generally considered to have a wide energy distribution. As a

result, surface coating-like films or droplets can be formed by deposition of particles with energies below the threshold value to cause subsequent sputtering of a new host substrate. This is also true for the sputter deposition or vapor deposition processes, which are standard film production techniques for micro-electronics purposes [6].

In contrast, the target is practically the only plasma interactive component in the PISCES facility. Also, the linearly magnetized plasma naturally flows to the target due to the pre-sheath electrostatic potential, which is approximately $-1.5kT_e/e$. It follows that reionized materials will be redeposited back on the original surface, guided by the magnetic and pre-sheath electrostatic fields. Consequently, the target is subject to simultaneous bombardment of the primary plasma ions and redepositing materials ions, each accelerated by the same sheath potential drop. In this case, redepositing ions will generally erode the target surface by self-sputtering. As will be shown later in detail, trapping of redepositing ions associated with the self-sputtering process plays an important role in determining the net erosion yield. However, these trapped ions will be removed by subsequent ion bombardment because of the short implantation depth shown in fig 2. Therefore, ordinary coating-like films can not be expected to grow from the redepositing materials in the PISCES facility.

4. MODELING OF EROSION AND REDEPOSITION OF MATERIALS

The first-order modeling of simultaneous erosion and redeposition of materials (the computer program, AREX; Analysis of Redeposition EXperiment) in the PISCES facility is outlined here for consistency although details can be found elsewhere[2]. Major mechanisms involved in this modeling include: (1) target sputtering by the primary plasma ions being accelerated by the negative sheath potential; (2) reionization of sputtered materials by electron impact; (3) trapping of material ions on the magnetic field lines and

transport back to the original target surface; and (4) self-sputtering of the target by the redepositing ions, accelerated by the same sheath potential as that for the primary plasma ions.

The sputtering yield and self-sputtering yield are calculated by Yamamura's analytic formula [9]. Velocities of sputtered particles are estimated from the well-known energy distribution [5]: $N(E)=E/(E+U_s)^3$, where U_s is the surface binding energy of the target material. The cross section of electron impact ionization is obtained from Lotz's formula [10] and then averaged over the Maxwellian energy distribution to estimate the rate coefficient. As an example, calculated mean free paths for electron impact ionization processes of sputtered copper and iron are shown in fig. 3.

The probability of redeposition is defined as the fraction of sputtered neutrals which will be ionized within the projected space of the target, assuming that the emission of sputtered particles obeys the cosine law. The probability of redeposition, β , as shown in fig. 4, decreases rapidly as the mean free path for electron impact ionization increases. Since the mean free paths for second and third ionization are appreciably long as shown fig.3, only redeposition associated with first ionization is considered in this model. Using this probability redeposition, the total erosion rate can be given by the following series:

$$dV/dt = Y_s(1-\beta) \left[1 + \{ Y_{ss} - (1-R) \} \sum_{n=0}^{\infty} (\beta Y_{ss})^n \right] \quad (1)$$

where Y_s and Y_{ss} are the sputtering yield due to the primary plasma ions and self-sputtering yield due to the redepositing ions, respectively. The term, R , is the particle reflection coefficient of redepositing ions, which can be calculated using the Monte Carlo program: TRIM[11]. Retention of implanted plasma ions is considered to be negligible compared with the total erosion of the target material. Also, the sputtering yield and self-sputtering yield are assumed to be independent of the surface morphology of the target.

Notice that when the probability of redeposition is negligibly small, the net erosion rate estimated by eq.(1) becomes essentially the same as the sputtering erosion due to the primary plasma ions. For a certain value of the probability of redeposition, terms after the second one of the series are negative if the self-sputtering yield due to redepositing ions is smaller than $(1-R)$, which is equivalent to the trapping coefficient. It follows directly from this that the resultant net erosion rate will be smaller than the classical sputtering erosion rate. Another important implication is that the 'run-away erosion' condition for the PISCES experiment is $\beta Y_{ss} > 1$, which is similar to that for a large toroidal device [12].

Although only physical sputtering cases are treated in this model, the concept of redeposition is common for both chemical and physical sputtering cases. Now, consider a typical ion-target combination to cause chemical sputtering such as hydrogen ion-carbon (graphite) interaction which often induces gaseous methane production [13]. The electron impact ionization rate coefficient for methane is comparable with that for carbon in the electron temperature range of the PISCES plasma [14]. However, methane molecules are considered to be released with thermal energies determined by the surface temperature. This implies that velocities of desorbing methane molecules are much smaller than those of physically sputtered carbon atoms. Therefore, one may well expect a short ionization mean free path and hence a high probability of redeposition for chemically sputtered products such as methane. Details of the graphite-hydrogen plasma interaction experimental data taken in the PISCES facility can be found elsewhere[15].

The experimental data for normalized erosion yields determined by the weight loss method are compared with the theory in fig.5. As theoretically predicted, the normalized erosion yield data are found to be significantly smaller than unity, which corresponds to the classical sputtering yield, when the mean free path for electron impact ionization becomes shorter than about 15 cm. There is generally agreement between the theory and data although further improvement needs to be done. The present theory tends to overestimate the net erosion yield, particularly in the redeposition dominated regime. Statistically, the

samples with strongly modified surface morphologies yield the data points which fall below the theory curve. This indicates some topographical retrapping effect of sputtered particles [6], which results in a reduction of the effective sputtering yield. This will be discussed later in detail.

5. SURFACE CHARACTERISTICS OF PLASMA BOMBARDED MATERIALS

It is widely recognized that surface characteristics of plasma interactive components of a magnetic fusion device can affect the entire scenario of operation of fusion devices. Among these surface characteristics, surface morphologies of redeposited materials and related issues have motivated the present study. Redeposited materials were characterized by various surface analysis techniques. These techniques include SEM, AES, SIMS, RBS, EMPA and conventional X-ray diffraction analysis. Some of the results out of these measurements are presented here.

5-1. SURFACE MORPHOLOGIES OF REDEPOSITED MATERIALS

Because of the high plasma flux utilized in the present study, the surface morphology is expected to change rapidly with time. The time evolution of surface morphologies of copper and 304 stainless steel (304SS) during Ar plasma bombardment has been investigated under typical redeposition conditions cited in table 1. The incident ion flux was set at 1.5×10^{18} and 1×10^{18} ions $\text{sec}^{-1}\text{cm}^{-2}$ for copper and 304SS, respectively. During the course of these experiments, the plasma parameters were controlled such that the mean free path for first ionization of sputtered materials is approximately 1.5

cm. The target temperature was set at 320K to eliminate thermal effects on the evolution of the surface morphology. These thermal effects will be described later.

The surface morphologies of redeposited copper and 304SS are shown in figs. 6 and 7, respectively. Generally, the surface appears to be deeply etched and some grains become relieved as the ion fluence increases. This illustrates the crystalline orientation effect on the sputtering yield [5]. A detail investigation of this effect is beyond the scope of the present study. Nevertheless, one important result drawn from these experiments is that the redeposited surface does not have any particular features when compared with an ordinary sputter etched surface. Our AES surface analysis showed that there are no major impurities on these redeposited surfaces. The bombarded 304SS samples indicated somewhat chromium enriched composition relative to as-polished samples. The detail will be published later.

During this series of experiments, the net erosion yield was determined by the weight loss method. The result is shown in fig. 8. Notice that the weight loss of the target increases linearly with increasing ion fluence. (The slope of the lines is approximately 45 degrees in the logarithmic plot.) It follows that the net erosion yield is independent of ion fluence so long as the surface morphology is not significantly modified from that of an ordinary sputtered surface. The resultant net erosion yields normalized to the corresponding classical sputtering yields are 0.3 and 0.15 for copper and 304SS, respectively. These net erosion yields are in a relatively good agreement with the theory utilizing Yamamura's formula [9] to estimate the sputtering yields (see fig. 5). This implies that the redeposited material in the PISCES facility has essentially the same sputtering yield as an ordinary bulk material.

5-2. EFFECT OF IMPURITIES ON SURFACE MORPHOLOGY

In a magnetic fusion device, a number of different surface materials are directly or indirectly facing the plasma. These materials are eroded by energetic particles, and can then be redeposited elsewhere as foreign impurities. In this section, the effect of foreign impurities on the surface modification under plasma bombardment is discussed in detail.

As a preliminary attempt, molybdenum from the electrode of the Langmuir probe was doped into the Ar-plasma stream. The molybdenum electrode was set at 100 V negative with respect to the plasma. A certain fraction of sputtered molybdenum atoms will be reionized and redeposited on the target surface positioned downstream (see fig.1). Under a typical redeposition condition having an argon ion flux of 10^{18} ions $\text{sec}^{-1}\text{cm}^{-2}$, the rate at which molybdenum atoms are deposited on the target surface is roughly estimated to be in the order of 10^{13} atoms $\text{sec}^{-1}\text{cm}^{-2}$. This is a few percent of the atomic density of a surface monolayer. The total deposition fluence of molybdenum is 10^{14} - 10^{15} atoms cm^{-2} .

The surface morphologies of copper and of 304SS bombarded by Ar-plasma doped with molybdenum are shown in figs. 9 and 10, respectively. Both copper and 304SS bombarded at ambient temperatures between 300 and 320K show similar surface morphologies to those shown in figs. 6 and 7, respectively. However, copper bombarded at temperatures generally above 400K shows densely populated cones, some of which have compound conical structures. Also, 304SS bombarded at temperatures above 500K generally shows a coral-like winding structure. Interestingly, these microscopic features can be visually identified by the color of the bombarded surface: sputter-etched surfaces retain their original metallic colors with glitters from relieved micro-grains whereas modified surfaces have much darker colors with a felt-like appearance. These results clearly indicate that the presence of molybdenum as a foreign impurity can significantly affect the surface modification processes at elevated temperatures but has little influence at ambient temperatures. A systematic investigation of the temperature effect is under way.

Unfortunately, there is no single theory to interpret all the impurity-induced surface morphologies. It is, however, generally considered that a surface impurity element, which has a lower sputtering yield than the substrate, can be a nucleus to induce protruding features [6]. One recent theory proposed by Wehner [16] indicates that the impurity acting as a seed to grow cones must have a higher melting point than the substrate. Such impurities can be either from an external source or from the bulk of the substrate. The seed-substrate combinations used in the present experiment: Mo-Cu and Mo-304SS meet the primary requirement for impurity-induced surface modification with respect to both the sputtering yield and melting point arguments.

The molybdenum-seeded cone structure on copper shown in fig. 9, (b) is quite similar to that found at 573K by Rosnagle and Robinson [17]. They indicate that the compound cone structure arises after the seeds or coatings are eroded by subsequent ion bombardment. In fact, our spot surface analysis by EMPA and AES failed to detect molybdenum on these cone-covered copper surfaces. However, a weak indication of molybdenum was found in the SIMS spectra shown in fig. 11. This analysis also found iron and chromium on both the copper surfaces, with and without cones. These extra impurities may be from some section of the vacuum chamber of the PISCES facility. However, it is deductively clear that the surface modification was not driven by these extra impurities under the present condition. Also, it is found by X-ray diffraction analysis that the sub-surface structure of the cone-covered copper retains the original FCC (Face Centered Cubic) crystalline structure. This is reasonable since the X-ray penetration depth, which is about 25 μm , is a few orders of magnitude larger than the region where the surface modification is taking place.

Generally, the winding structures are found for copper surfaces seeded with tungsten at high temperatures. These features are often attributed to a flow or agglomeration of the coating material between adjoining cones [18]. However, the coral-like winding structure found on the redeposited 304SS presented in fig. 10 appears to have

more complex structure in a tilted view. This clearly indicates a different mechanism. Because of the poor thermal conductivity of 304SS, local temperatures at sharp tips of seed cones can be appreciably higher than the bulk temperature. Some quasi-liquid state [18] might be attained. Possible consequences are that these quasi-melted cone tips will bend and eventually bridge each other to create the coral-like features. Further investigation needs to be done to clarify the mechanism. RBS analysis was conducted for redeposited 304SS using a 6MeV He⁺ ion beam. The result indicates that the concentration of molybdenum is about 1×10^{16} atoms cm⁻² in the surface region with a thickness of about 2 μ m. Also, the spot analysis by EMPA found molybdenum both on the ridges and in the valleys of the winding structure. The characteristic X-ray spectra are shown in fig 12. Also, the modified surface at an elevated temperature indicated chromium enriched composition relative to that for the as-polished surface. However, this is not surprising since stainless steels often segregate chromium at elevated temperatures in vacuum [19]. One difficulty in surface analysis is that seed materials may be largely eroded, once strong surface modification begins.

The substrate temperature is also a key parameter affecting surface modification for a given seed-substrate combination since seeds must migrate via surface diffusion to form an effective impurity cluster or local coating to induce a protuberance [20,21]. This means that the processes of forming such an impurity cluster and erosion of individual seeds under ion bombardment are competitive one another. It follows that there is a critical temperature to trigger the surface texturing for a given seed concentration. Opposite is also true, namely, the minimum seed concentration exists for a given temperature. The minimum seed concentration has been found to be as small as a few percent of the atomic density of a monolayer [22]. Our EMPA analysis shown in fig. 12 provides us a convincing result of this thermal effect that no molybdenum was indicated on the redeposited 304SS seeded at an ambient temperature. Apparently, the surface diffusion

was defeated by sputter erosion of seeds in this kinetic competition governing the surface evolution, which resulted in the smooth surface morphology shown in fig. 10, (a).

The critical temperature for surface modification of copper by seeding molybdenum has been reported to be 470K under Ar ion bombardment with a flux in the order of 10^{16} ions $\text{sec}^{-1}\text{cm}^{-2}$. This critical temperature is somewhat higher than our finding: about 400K. Unfortunately, the discrepancy in these critical temperatures can not be clearly explained at present. There is a theory claiming that the ion bombardment enhances surface diffusion of impurity atoms [17]. This suggests a possibility that the critical temperature might be lower at a higher ion bombarding flux. Considering the high plasma flux in the present study, the relatively low critical temperature may not be surprising. However, the detail mechanism is still unclear.

In one experiment, the 304SS target temperature was changed from 300 to 650K at a ramp-up speed of roughly 30 degrees sec^{-1} to witness surface modification starting at the critical temperature. At about 550K, the surface morphology suddenly changed, which was visually identified by the color of the target through a viewing port. This sudden change will be theoretically interpreted later in this paper. The resultant modified surface morphology is similar to that shown in fig. 10, (b) and (c).

One remaining question is whether or not the initial surface contaminations such as oxygen and/or carbon, which are always detected by AES surface analysis, can be such an impurity as to induce protruding features. A tentative answer is negative unless there are strongly segregated oxide and/or carbide phases that can meet the requirements for seed materials. Interestingly, recent measurements [23] have shown a significantly reduced erosion yield for sputter-deposited copper. This was attributed to surface chemical compounds such as copper oxides formed during deposition. Further investigation is greatly anticipated in order to clarify this point.

5-3. MODELING OF IMPURITY DRIVEN SURFACE EVOLUTION

A simple model is introduced here to describe the surface modification by plasma bombardment although there are other elaborate theories for ion bombardment surface modification[6]. As described in section 3, the surface morphological evolution is driven mostly by physical sputtering under the PISCES plasma bombardment conditions. Again, simultaneous erosion and redeposition is equivalent to the bombardment of two different ions with the same energy (assuming the same degree of ionization).

The sputtering yield is well known to change with angle of ion incidence. This angular dependence is considered to be one of the crucial factors determining the surface modification process. As an example, the angular dependence of the sputtering yields of copper by argon and copper ions is shown in fig. 13. Notice that there is no significant difference in the angular dependence for these two cases. This suggests that the simultaneous erosion and redeposition of copper under argon plasma bombardment can be simply approximated as ion bombardment at an effective erosion rate given by the theory: AREX described in section 4.

Consider only the longitudinal motion of microscopic points on a material surface being modified by energetic ion bombardment. The longitudinal position, y , is expressed as a function of time, t , and lateral position, x :

$$y(x, t + \Delta t) = y(x, t) - \Delta y(x). \quad (2)$$

The recession rate due to the ion bombardment, Δy , is determined by

$$\Delta y(x) = dIY(\theta)\Delta t \quad (3)$$

where d is the monolayer thickness of the target material, I is the incident ion flux, and Y is the effective erosion yield as a function of angle of incidence, θ . The angular dependence of the effective erosion yield can be obtained from a TRIM calculation [11], as shown in fig.13. The product of these two factors is assumed to give a net erosion rate determined by eq.(1). The angle of incidence with respect to the surface normal is equal to the slope of the surface contour and is given by

$$\theta(x,t) = \tan^{-1}[\{y(x+\Delta x,t) - y(x-\Delta x,t)\} / 2\Delta x]. \quad (4)$$

At the surface impurity spot, x' , the longitudinal recession rate is

$$\Delta y(x') = d' Y'(\theta) \Delta t \quad (5)$$

where d' and Y' is the monolayer thickness and sputtering yield of the seed material, respectively. The incident angle will be set at zero for an impurity-seeded spot.

Another mechanism involved in this model is retrapping of sputtered particles to bury deep valleys between protruding features. This can be simulated by setting the recession rate equal to zero at the bottom point of a steep valley having slopes for which the sputtering yield is zero. In this preliminary version, however, quasi-liquid states are not considered.

As an example, the time evolution of a copper cone seeded with molybdenum under Ar-plasma bombardment was simulated using this model. In this example, the initial surface is assumed to be flat for simplicity. The flux and energy of the Ar-plasma bombardment are set at 1.0×10^{18} ions $\text{sec}^{-1} \text{cm}^{-2}$ and 100 eV, respectively. The redeposition conditions are assumed to give a net erosion yield of 0.3 normalized to the corresponding sputtering yield. An impurity cluster with a thickness of 300 angstroms is located at the center of the simulated surface: $x=0$. This hypothetical thickness of the

impurity cluster was set such that the seed material will be eroded in the course of simulation.

The result is shown in fig. 14. One can realize that the growth of the molybdenum-seeded cone is quite rapid under these conditions. This is consistent with our experimental finding of the sudden change of the surface morphology of 304SS induced by seeding molybdenum at an elevated temperature. Also, a compound cone structure such as that shown in fig. 9, (b) is theoretically found after the seed material is eroded. These results indicate that this first-order modeling can be at least qualitatively compared with the present experimental data.

6. FUSION RELATED SURFACE PROPERTIES OF RFDEPOSITED MATERIALS

6-1. SPUTTERING YIELD OF REDEPOSITED MATERIAL

The strongly modified surface morphologies with a coral-like winding structure (fig. 10, (b) and (c)) and densely populated, tall cone structure (fig 9, (b)) indicate a possibility that sputtered particles can be retrapped within these surface features. In order to check this possibility, the sputtering yield of redeposited copper with cones was measured using a deuterium (D^+) ion beam at an energy of 200 eV. As shown in fig. 15, the resultant sputtering yield of copper with cones was found to be reduced by a factor of two relative to that with a smooth surface. Recently, Auciello reviewed both experimental and theoretical studies on the retrapping behavior of textured surfaces [24]. It was pointed out that the sputtering yield of a surface with densely populated cones is likely to be reduced, particularly in the low energy range from 200 to 4000 eV. This is quite consistent with our experimental finding of the reduced sputtering yield of redeposited copper with molybdenum seeded cones.

As a first-order attempt, the theory: AREX was modified such that the modified surface has a 50% reduced sputtering yield. The result is shown by a dotted line in fig. 5. Apparently, the observed discrepancy between the theory and experimental data is compensated by this modification. However, further investigation needs to be done, given the scatter in the experimental points.

It is of considerable importance to note here that a decade ago, an artificial honeycomb structure was once proposed and demonstrated as a surface texture for first walls to minimize material erosion[25, 26]. The experimental findings mentioned above clearly indicate a possibility that one may expect a "natural honeycomb structure" on surface components of an operating fusion device.

6-2. DEUTERIUM REEMISSION, RETENTION AND PLASMA DRIVEN PERMEATION

From a practical engineering point of view, of great interest is to investigate fusion related characteristics of redeposited materials with strongly modified surface morphologies. Deuterium reemission, retention and plasma driven permeation were measured for redeposited 304SS with a coral-like surface structure. The techniques for these measurements are described in detail elsewhere[27,28,29].

The surface roughness of the redeposited 304SS was quantified by the BET (Brunauer, Emmett, Teller) method. The result indicated increased surface area for the redeposited 304SS by a factor of about 10, which in turn is similar to that for the surface modified by helium blisters [30].

The deuterium reemission measurement was conducted at an ambient temperature using a 6 keV D^+_3 beam with a flux of 2×10^{14} D $\text{sec}^{-1}\text{cm}^{-2}$. The targets were first bombarded up to a fluence in the order of 10^{18} D cm^{-2} until a reproducible reemission

response was observed during beam-on/off cycles. Because of the small sputtering yield for deuterium, the surface modification during this pre-treatment process is negligible compared with the original modification. The result of reemission measurements is shown in fig. 16. Deuterium reemission from redeposited stainless steel is increased by a factor of 2 relative to as-received materials under identical conditions. Also, the rise and decline of reemission for the redeposited target is somewhat faster than those for as-received materials. This behavior is quite similar to the case when the surface is deliberately roughened before ion implantation [27].

At temperatures below 370K, deuterium reemission is generally controlled by solid-state diffusion kinetics [27]. Because of the strongly modified surface, a significant fraction of incident deuterium ions impinge on the target at grazing angles in the coral structures. Therefore, the depth distribution of implanted ions for the modified surface is considered to be effectively shallower than that for a flat surface. It follows that the diffusion length required to release deuterium is short, which results in an increase in the reemission ratio.

Using the NRA method [28] based on the reaction, $D(^3\text{He},p)^4\text{He}$, deuterium retention in the near surface region (about 1 μm below surface) was measured after implantations up to a fluence of 10^{18} D cm^{-2} . The result showed deuterium concentrations of 3×10^{16} and 8×10^{15} D cm^{-2} for the near surface region with a depth of about 1 μm of the redeposited and as-received materials, respectively. This result implies that a strongly modified surface tends to reflect the bombarding particles because of the grazing angle of incidence.

Plasma driven permeation of deuterium through redeposited 304SS was measured at 823K using the TPX (Tritium Permeation Experimental) facility [29]. The modified surface was placed facing the deuterium plasma. The plasma bombardment current density was 0.5 nA cm^{-2} . The sample was set at 25V negative to the plasma so as not to make further surface modification due to sputtering by the deuterium plasma bombardment

during permeation measurement. The result obtained is shown in fig.17. The steady state permeation rate through the redeposited material was found to be reduced by a factor of 2 to 3 relative to the as-received material. In this temperature range, deuterium reemission is generally controlled by molecular recombination at the surface. Therefore, it can be concluded that the decrease in the steady state permeation rate is due to the increased surface area which in turn leads to an increase in deuterium desorption in the upstream. The reduction of plasma driven permeation is favorable for fusion engineering from a tritium handling safety point of view.

7. CONCLUSIONS

Surface modification of materials by continuous plasma bombardment has been investigated under simultaneous erosion and redeposition conditions. The mechanism of redeposition is analyzed to evaluate the net erosion yield. The erosion rate due to the plasma bombardment significantly decreases, when redeposition occurs, so long as the self-sputtering yield is smaller than the particle trapping coefficient. The morphology of the surface subject to simultaneous erosion and redeposition is found to be similar to that of an ordinary sputter-etched surface. Also, the redeposited material indicates essentially the same sputtering yield as a bulk material. However, the presence of impurities can significantly modify the surface morphology and sputtering behavior. The mechanism of impurity-induced surface evolution is theoretically elucidated. Also, the critical temperature for impurity-induced surface modification is found to be about 400K and 550K for copper and 304 stainless steel, respectively. Strongly modified surface morphologies result in a reduction of the sputtering yield by the subsequent ion bombardment. Due to the increased surface area of a modified surface lead to an increase in gas reemission and hence a decrease in plasma driven permeation.

Of particular importance to the fusion community is the finding that plasma interactive surfaces can be strongly modified by foreign impurities transported from different components. A "natural honeycomb structure" to reduce the erosion rate as well as tritium permeation can be developed in an operating fusion device. However, properties of redeposited surfaces investigated in the present work might be different from those of coating-like deposits. Further investigation is necessary to understand the nature of surfaces redeposited differently.

ACKNOWLEDGEMENT

The X-ray diffraction analysis by L.Keller is greatly appreciated. The authors wish to acknowledge the technical support by T.Sketchley and V.Low. Special thanks go to K.Andrews for his dedicated work on the computer data acquisition system of the PISCES facility. This work is supported by the United States Department of Energy, Office of Fusion Energy under contract #DE-AT03-84ER52104.

Table 1. Experimental Parameters for Typical Redeposition Conditions.

Parameters	Copper	304 SS
Ion Bombardment Energy(eV)	100	100
Sputtering yield(atoms ion ⁻¹)	0.43	0.21
Self-sputtering yield(atoms ion ⁻¹)	0.395	0.188
Particle reflection coefficient	0.197	0.213
Ion Flux(Ar ⁺ sec ⁻¹ cm ⁻²)	1.5 x10 ¹⁸	1.0 x10 ¹⁸
Electron temperature(eV)	10.6	15.5
Electron Density(cm ⁻³)	5.96x10 ¹²	3.11x10 ¹²
Mean Free Path (cm)	1.49	1.46

REFERENCES

- [1] D.E.Post and R.Behrisch, *Physics of Plasma-Wall Interactions in Controlled Fusion*, Plenum Press (1986).
- [2] Y.Hirooka, D.M.Goebel, W.K.Leung, G.A.Campbell and R.W.Conn, to be published in *J.Nucl. Mater.* (presented at 2nd Int.Conf.Fusion Reactor Materials, Chicago, 1986).
- [3] D.M.Goebel, G.A.Campbell and R.W.Conn, *J.Nucl.Mater.* 121(1984)277.
- [4] D.M.Goebel and R.W.Conn, *J.Nucl.Mater.* 128 & 129(1984)249.
- [5] R.Behrisch, *Sputtering by Particle Bombardment*, Vols. 1&2, Springer-Verlag Berlin Heidelberg (1981 & 1983).
- [6] O.Auciello and R.Kelly, *Ion Bombardment Modification of Surfaces*, Elsevier Science Publishing(1984).
- [7] R.A.Langley, J.Bohdansky, W.Ecstein, P.Mioduszewski, J.Roth, E.Taglauer, E.W.Thomas and H.Verbeek, K.L.Wilson, *Nucl.Fusion Spec.Issue* 1984.
- [8] For example, P.Staib, H.Kukral, E.Glock and G.Staudenmaier, *J.Nucl.Mater.* 111&112 (1982) 173.
- [9] N.Matsunami, Y.Yamamura, Y.Itikawa, N.Itoh, Y.Kazumata, S.Miyagawa, K.Morita, R.Shimizu and H.Tawara, *Atom.Data and Nucl. Data Tables* 31(1984)1.
- [10] W.Lotz, *Z.Physik* 206(1967)205.
- [11] J.P.Biersack and L.G.Haggmark, *Nucl.Instr. & Methods*, 121(1980)257.
- [12] INTOR Report Phase-1, IAEA(1983).
- [13] For example, E.Vietzke, K.Flaskamp and V. Philipps, *J.Nucl.Mater.* 111(1982)763.
- [14] W.D.Langer, *Nucl. Fusion* 22(1982)751.
- [15] D.M.Goebel, Y.Hirooka, R.W.Conn, W.K.Leung, J.Bohdansky, K.L.Wilson, W.Bauer, R.A.Causey, A.E.Pontau, A.R.Krauss, D.M.Gruen, and M.H.Mendelsohn, to be published in *J.Nucl.Mater.* (presented at 7th Int.Conf. Plasma Surface Interactions, Princeton, 1986.).

- [16] G.K.Wehter, *J.Vac.Sci.&Technol-A*, 3(1985)1821.
- [17] S.M.Rossnagel and R.S.Rosinson, *J.Vac.Sci.Technol.* 21(1982)790.
- [18] S.M.Rossnagel and R.S.Rosinson, *J.Vac.Sci.Technol.* 20(1982)506.
- [19] A.Mathewson and M.H.Acjard, *Proc.7th Int.Vacuum Congr. and 3rd Int. Conf.Solid Surfaces*, Vol.2, Vienna (1977)1217.
- [20] S.M.Rossnagel and R.S.Rosinson, *J.Vac.Sci.Technol.* 20(1982)195.
- [21] H.Kaufman and R.S.Robinson, *J.Vac.Sci.Technol.* 16(1979)175.
- [22] S.M.Rossnagel and R.S.Robinson, *Rad.Eff.Lett.* 58(1981)11.
- [23] B.Bastasz, R.A.Kerst and R.A.Causey, *J.Nucl.Mater.* 122&123(1984)1421.
- [24] O.Auciello, *Rad.Effects* 60(1982)1.
- [25] S.N.Cramer and E.M.Oblow, *Nucl.Fusion*115(1975)339.
- [26] K.Ohta, H.Maeda, S.Yamamoto, M.Nagai, H.Ohtsuka, S.Kasai, Kodajima, H.Kinuma, S.Sengoku and Y.Shimonura, *J.Nucl.Mater.* 76(1987)489.
- [27] K.L.Wilson and M.I.Baskes, *J.Nucl.Mat.* 111&112(1982)622.
- [28] A.E.Pontau, M.I.Baskes, K.L.Wilson, L.G.Haggmark, J.Bohdansky, B.M.U.Scherzer and J.Roth, *J.Nucl.Mat.* 111&112(1982)651.
- [29] R.A.Causey, R.A.Kerst and B.E.Mills, *J.Nucl.Mater.* 122&123(1984)1547.
- [30] K.L.Wilson, A.E.Pontau, L.G.Haggmark M.I.Baskes, J.Bohdansky and J.Roth *J.Nucl.Mater.* 111&112(1982)622.

FIGURE CAPTIONS

- Fig. 1: A schematic diagram of the experimental arrangement.
- Fig. 2: A typical ion implantation profile calculated by the Monte Carlo program : TRIM [11]. In this case, Ar⁺ and Cu⁺ ions with an energy of 100 eV are assumed to be impinging on Cu.
- Fig. 3: Calculated ionization mean free paths for physically sputtered copper and iron under a typical plasma bombardment condition with an Ar ion: flux of 1.0×10^{18} ions sec⁻¹ cm⁻².
- Fig. 4: Calculated probability of redeposition of materials in the PISCES-facility.
- Fig. 5: Comparison of the theory: AREX and experimental data of the net erosion yield as a function of first ionization mean free path. The theory curve represented by a solid line assumes no retrapping effect and the curve represented by a dotted line assumes 50% reduced sputtering yield due to a topographical retrapping effect (see text).
- Fig. 6: Surface evolution of copper during Ar-plasma bombardment with an ion flux of 1.5×10^{18} ions sec⁻¹ cm⁻² under a simultaneous erosion and redeposition condition. The total ion fluences are: 4.53×10^{19} ions cm⁻² for (a), 9.33×10^{19} ions cm⁻² for (b), 2.8×10^{21} ions cm⁻² for (c), 9.06×10^{20} ions cm⁻² for (d), 1.81×10^{21} ions cm⁻² for (e), and 4.4×10^{22} ions cm⁻² for (f).
- Fig. 7: Surface evolution of 304 stainless steel during Ar-plasma bombardment with an ion flux of 1.0×10^{18} ions sec⁻¹ cm⁻² under a simultaneous erosion and redeposition condition. The total ion fluences are: 2.94×10^{20} ions cm⁻² for (a), 6.11×10^{20} ions cm⁻² for (b), 1.14×10^{21} ions cm⁻² for (c), and 2.81×10^{22} ions cm⁻² for (d).
- Fig. 8: The weight loss of the target as a function of total ion fluence.
- Fig. 9: Surface morphologies of copper bombarded by Ar-plasma doped with molybdenum seeds at an ambient temperature (a) and elevated temperature (b).
- Fig. 10: Surface morphologies of 304 stainless steel bombarded by Ar-plasma doped with molybdenum seeds at an ambient temperature (a) and elevated temperature: an overhead view (b) and a 30 degree tilted view (c).
- Fig. 11: Typical SIMS spectra from copper with (bottom) and without (top) seed-cones.
- Fig. 12: Typical EMPA spectra from 304 stainless steel with a relatively smooth surface (seeded at about 300K) and a coral-like winding structure (seeded at about 510K). Also, the spectra for as-received material are shown (top) for comparison.
- Fig. 13: The normalized sputtering yield of copper by 100eV Ar⁺ and Cu⁺ as a function of angle of incidence. Calculated sputtering yields by the TRIM code [11] are normalized to that for the normal incidence.

- Fig. 14: A simulation of the surface contour evolution of copper with molybdenum seeds during Ar-plasma bombardment under simultaneous erosion and redeposition.
- Fig. 15: The sputtering yield of redeposited copper. The closed square symbols represent the data from copper with a cone-covered surface and open square symbols represent those from copper with a smooth surface.
- Fig. 16: Deuterium reemission from redeposited 304 stainless steel with a modified surface morphology (a coral-like structure).
- Fig. 17: Plasma driven permeation of deuterium through redeposited 304 stainless steel with a modified surface morphology (a coral-like structure).

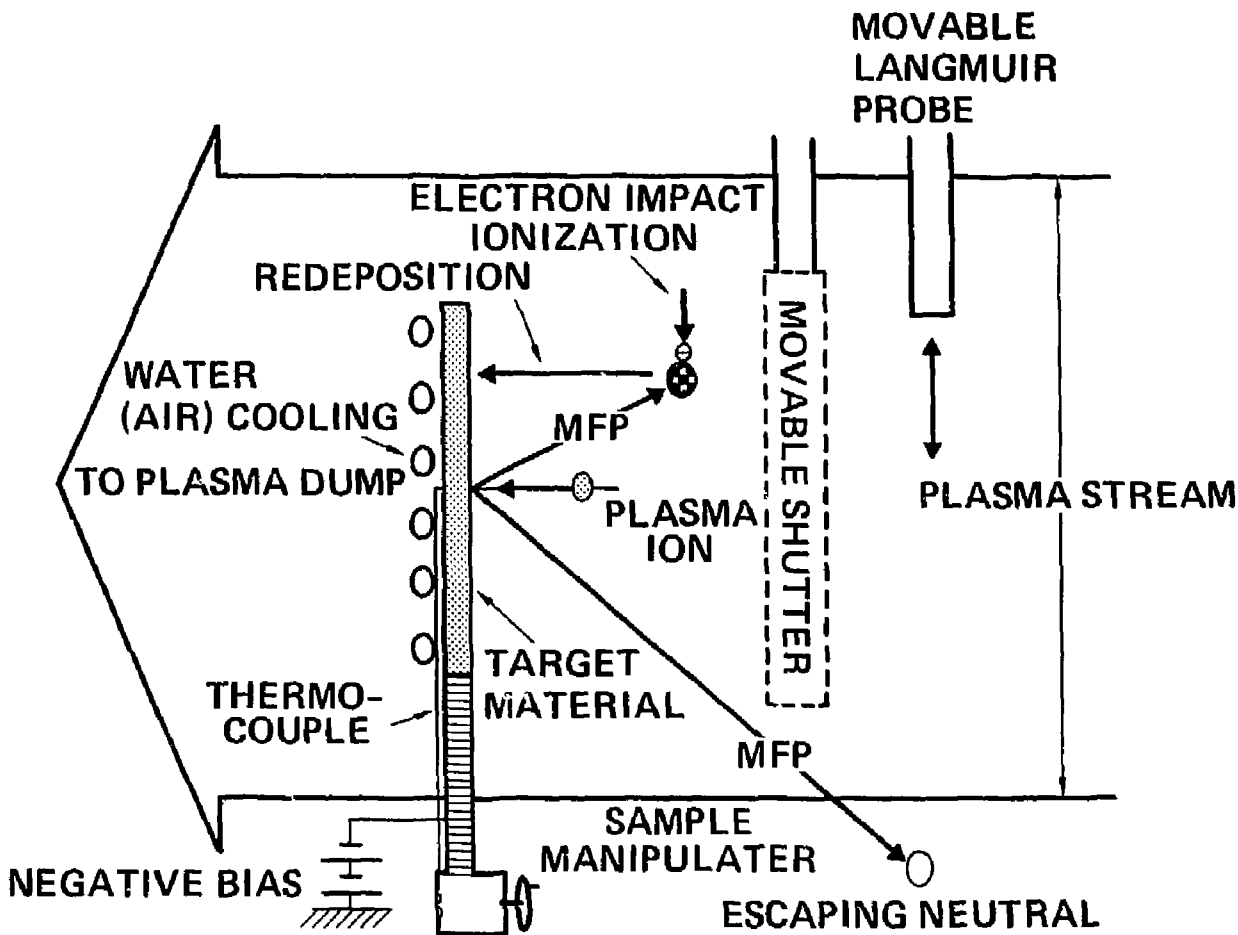


FIGURE 1

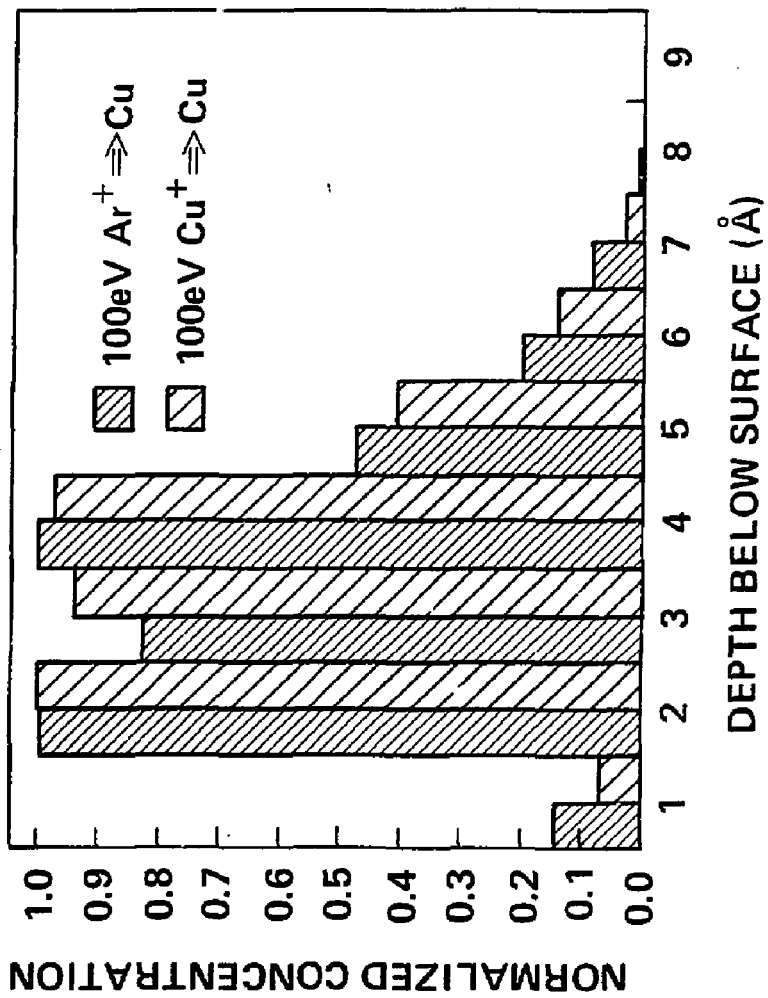


FIGURE 2

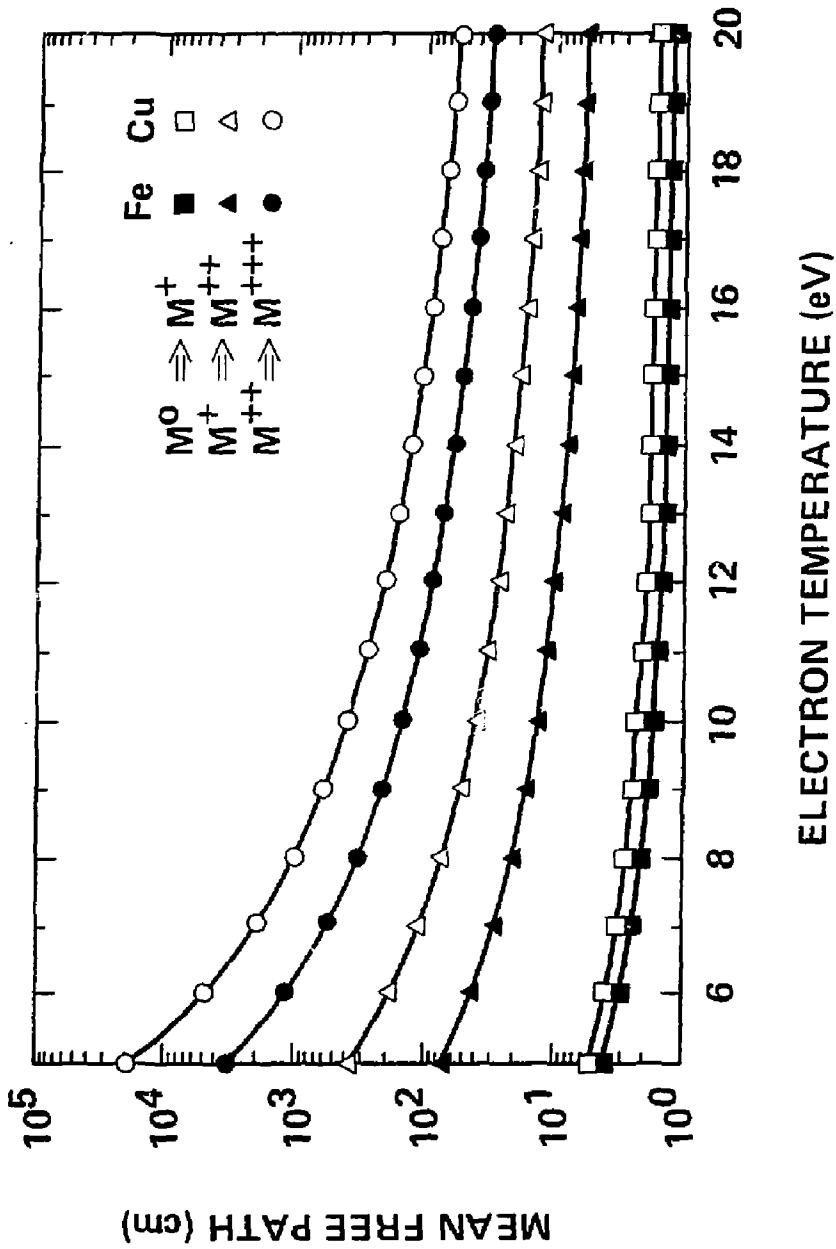


FIGURE 3

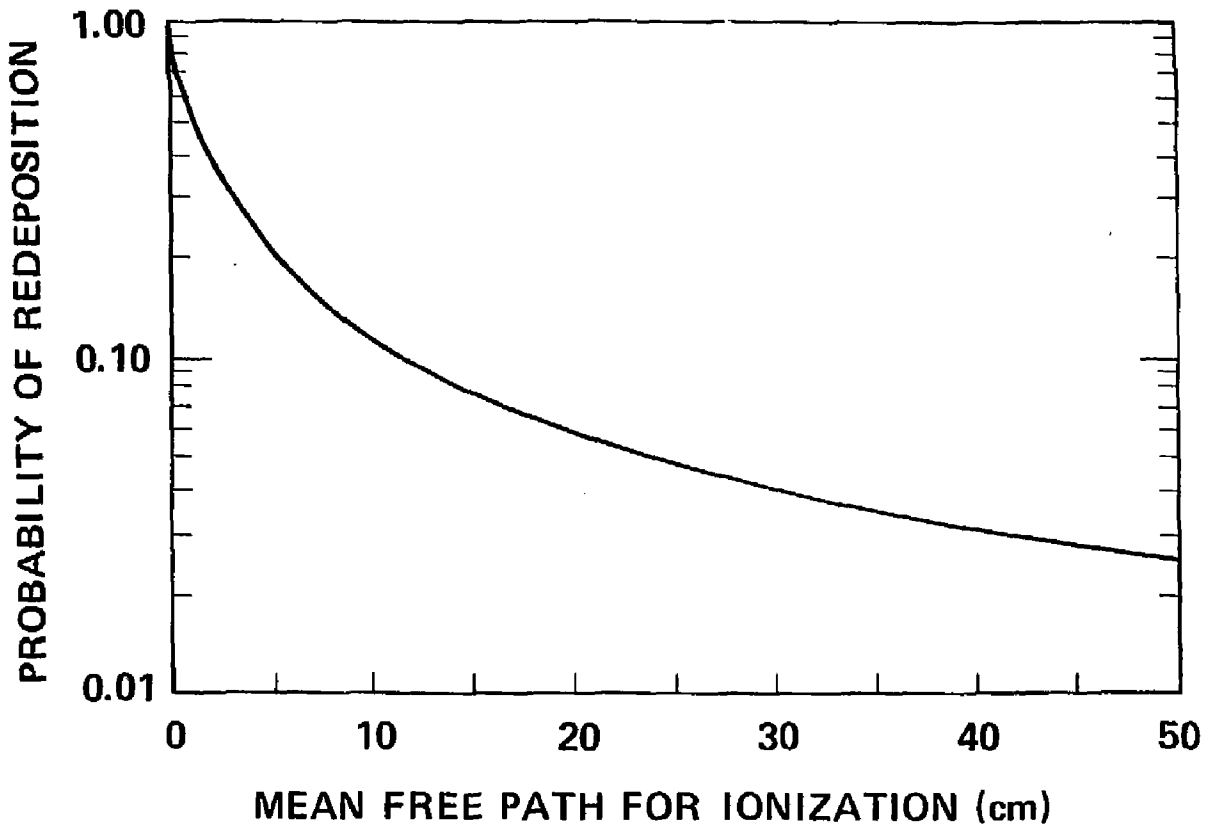


FIGURE 4
29

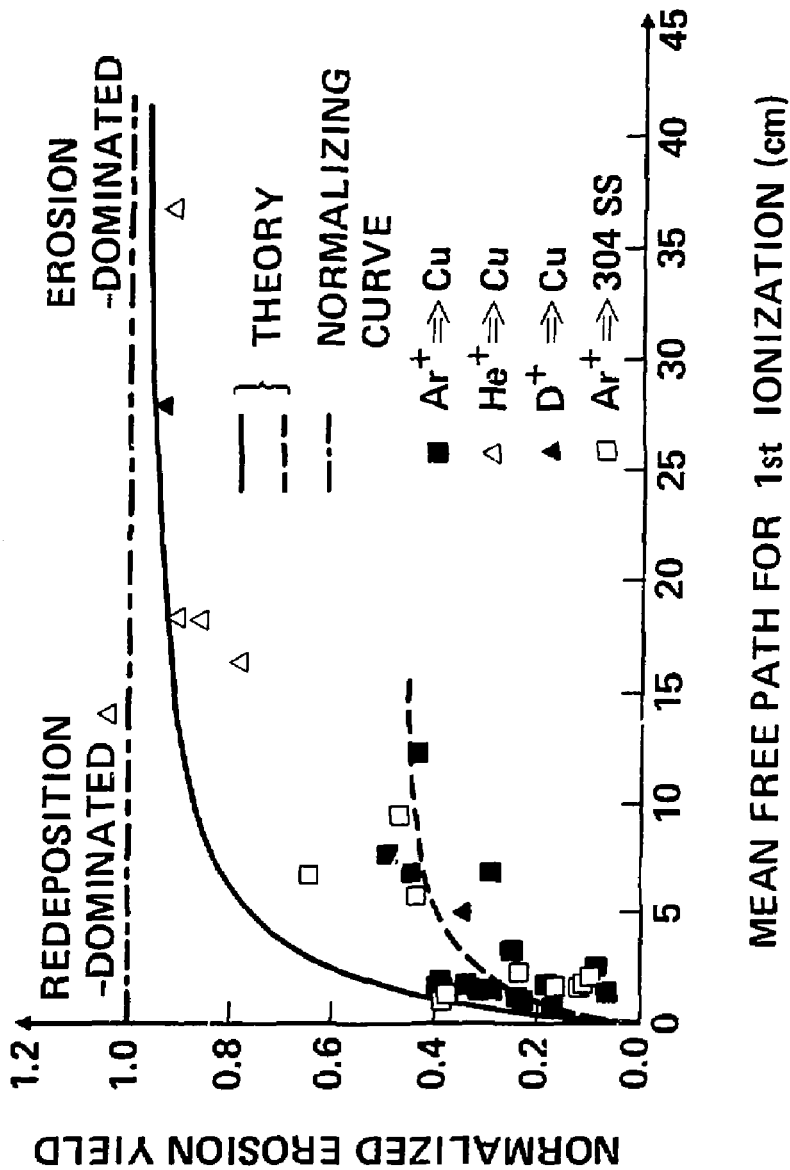
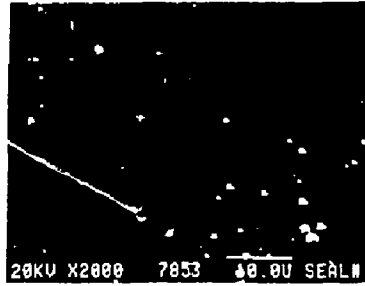


FIGURE 5



(a)



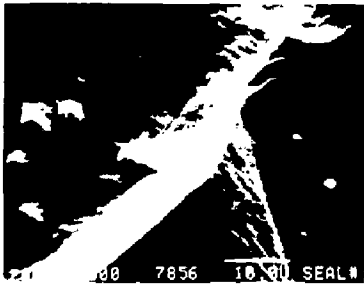
(b)



(c)



(d)



(e)



(f)

FIGURE 6



(b)



(d)



(a)



(c)

FIGURE 7

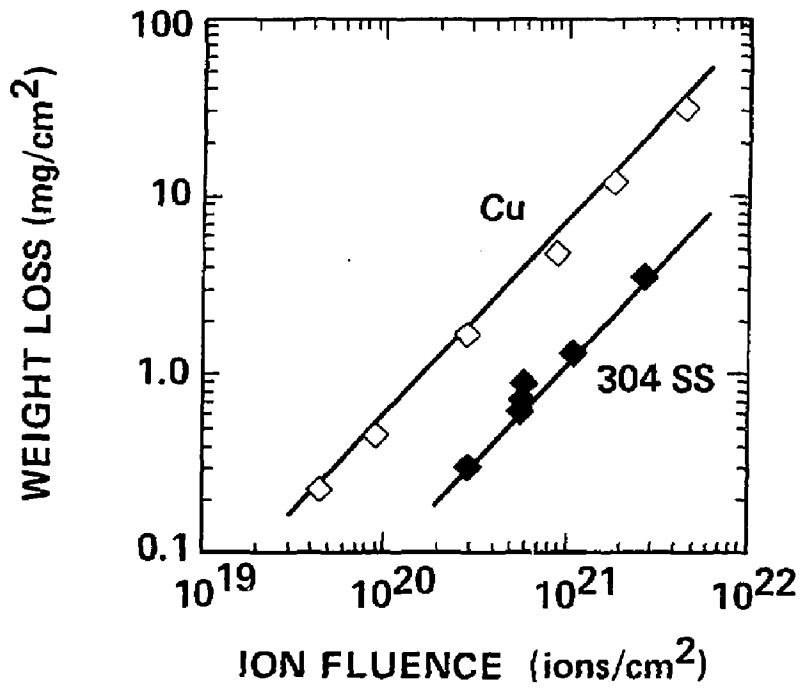
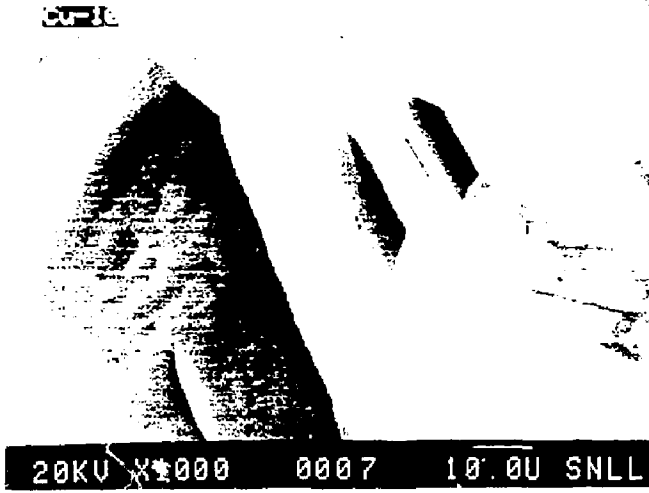
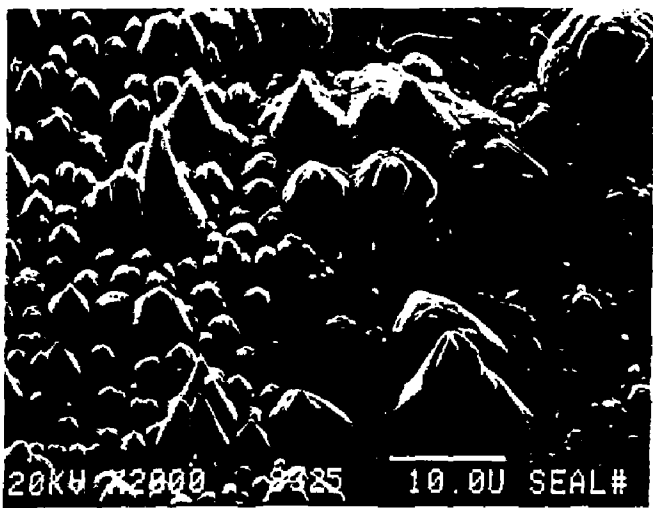


FIGURE 8



(a)

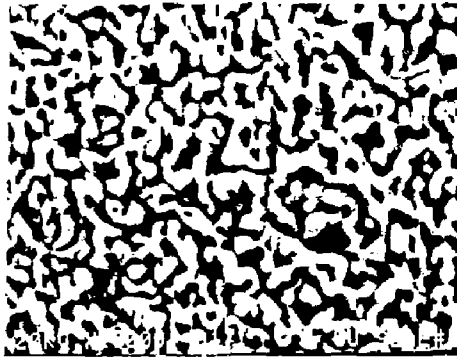


(b)

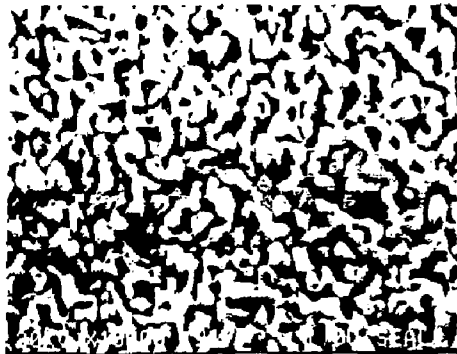
FIGURE 9



(a)



(b)



(c)

FIGURE 10

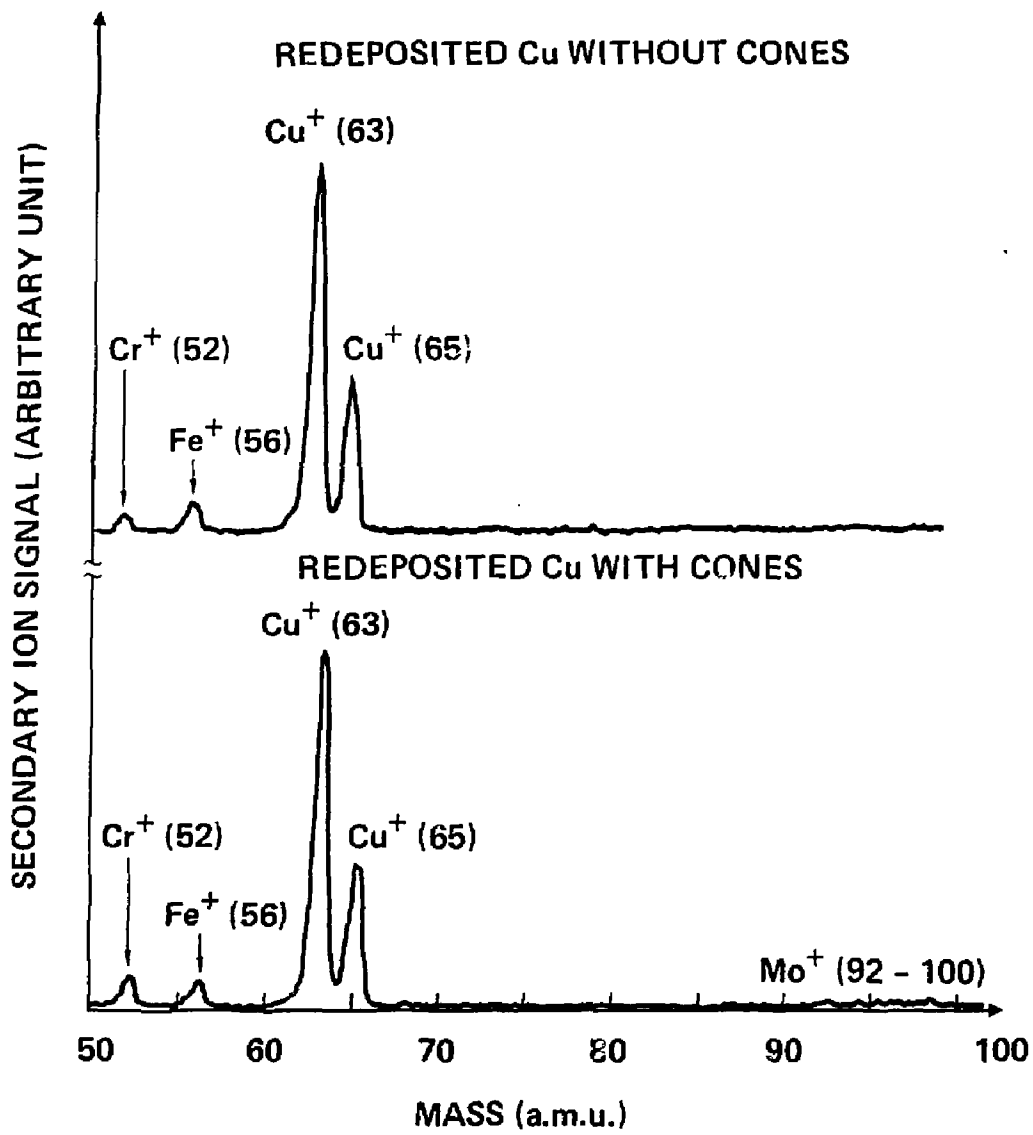


FIGURE 11

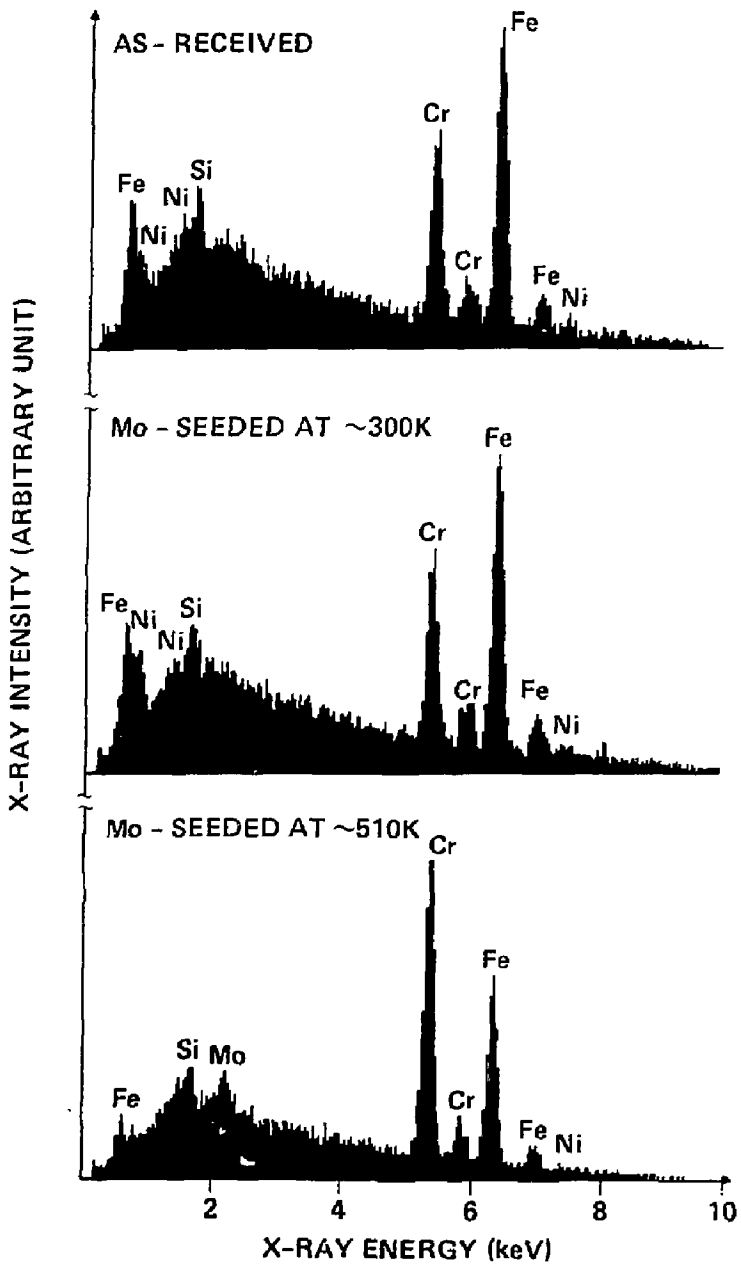


FIGURE 12

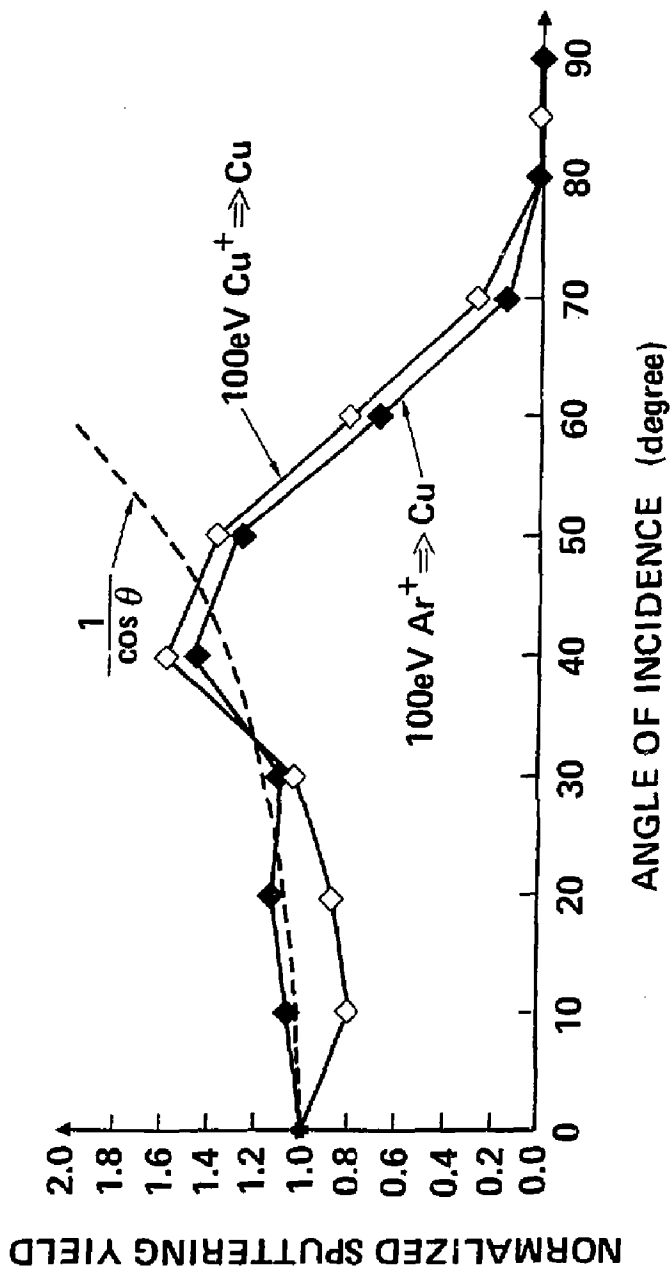
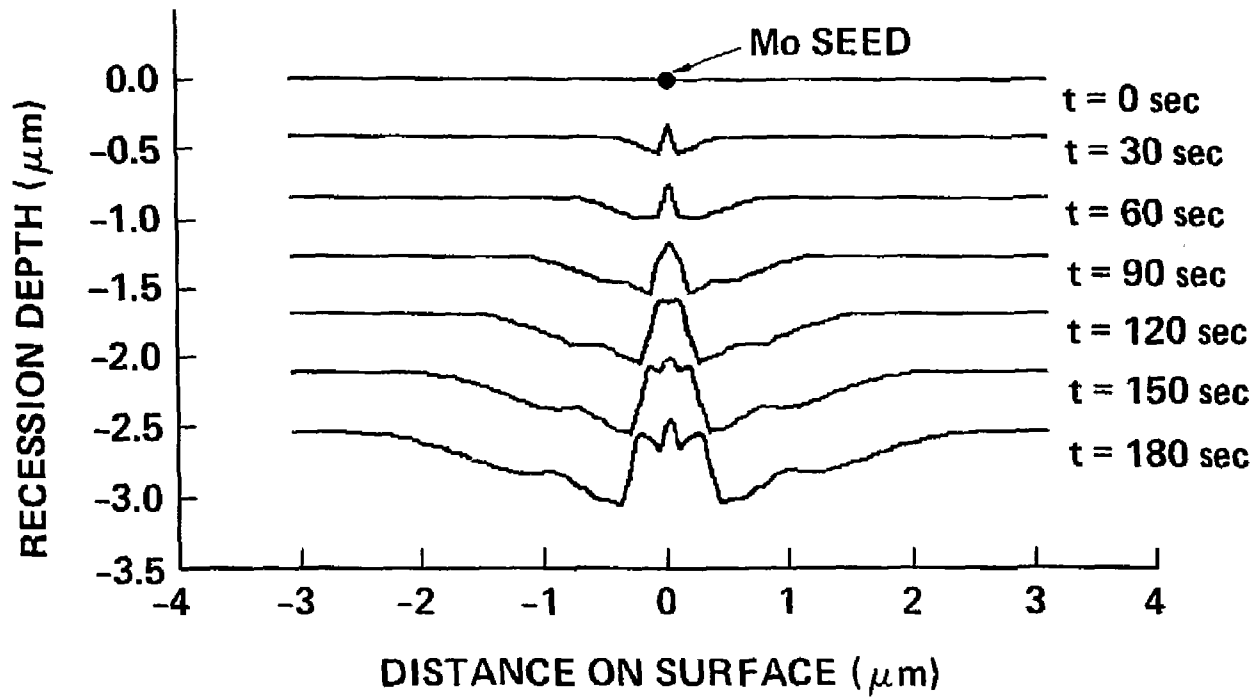


FIGURE 13

FIGURE 14



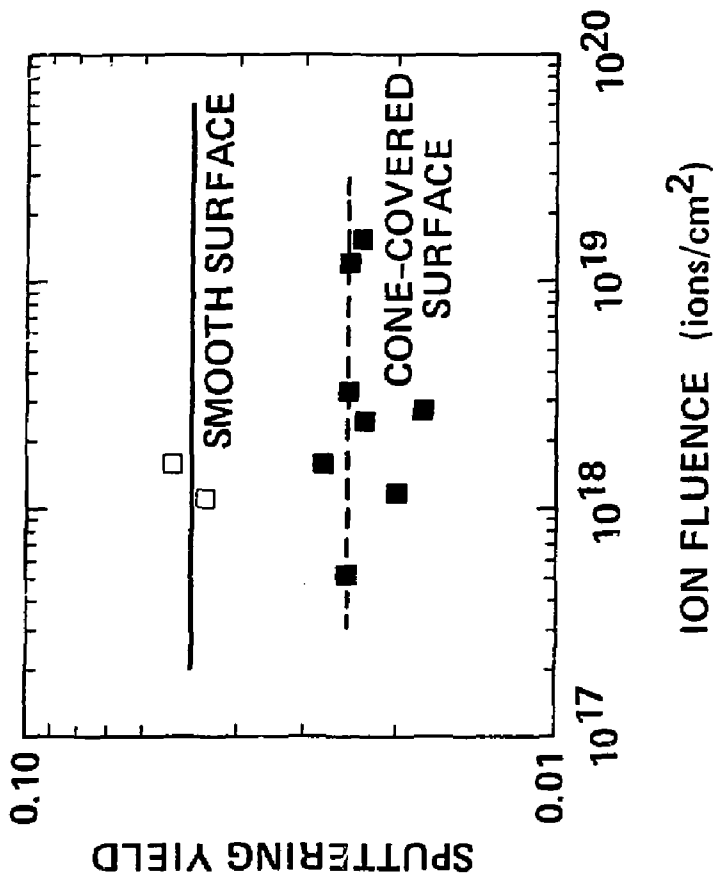


FIGURE 15

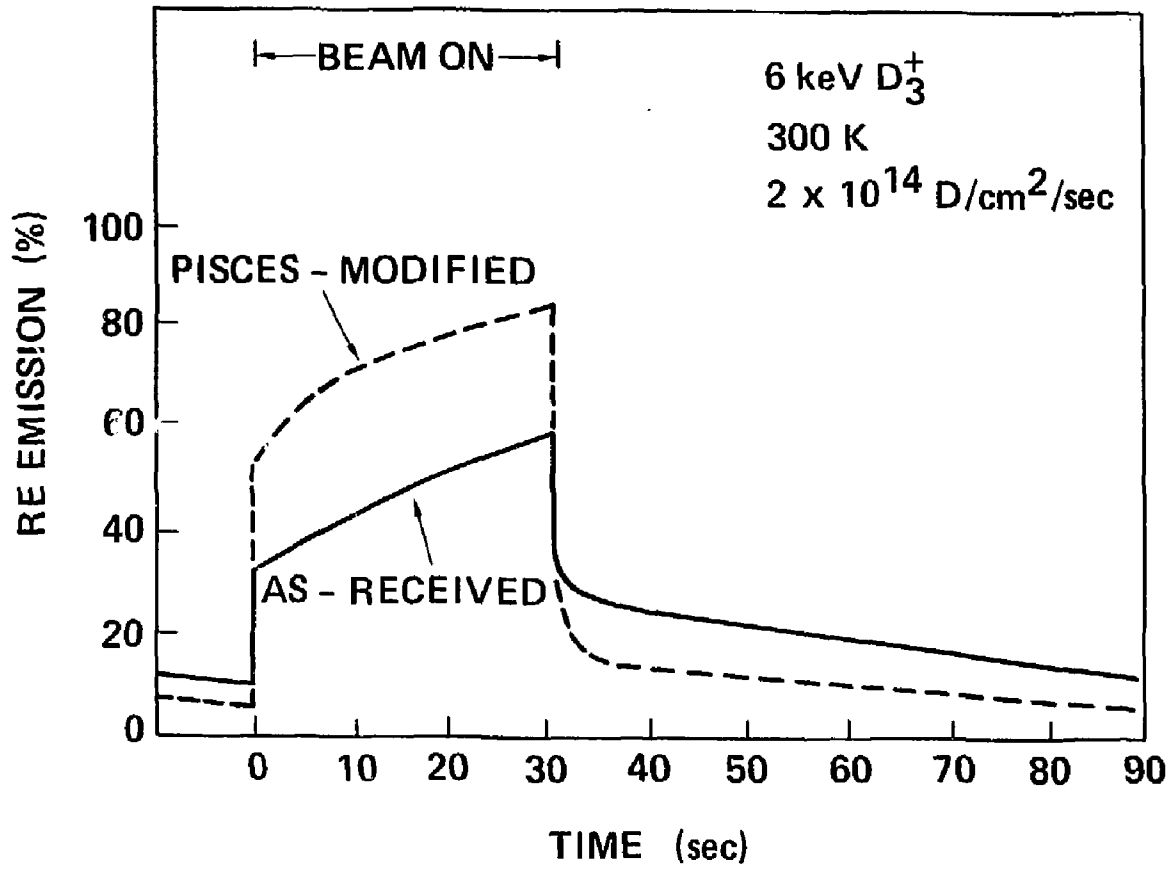


FIGURE 16

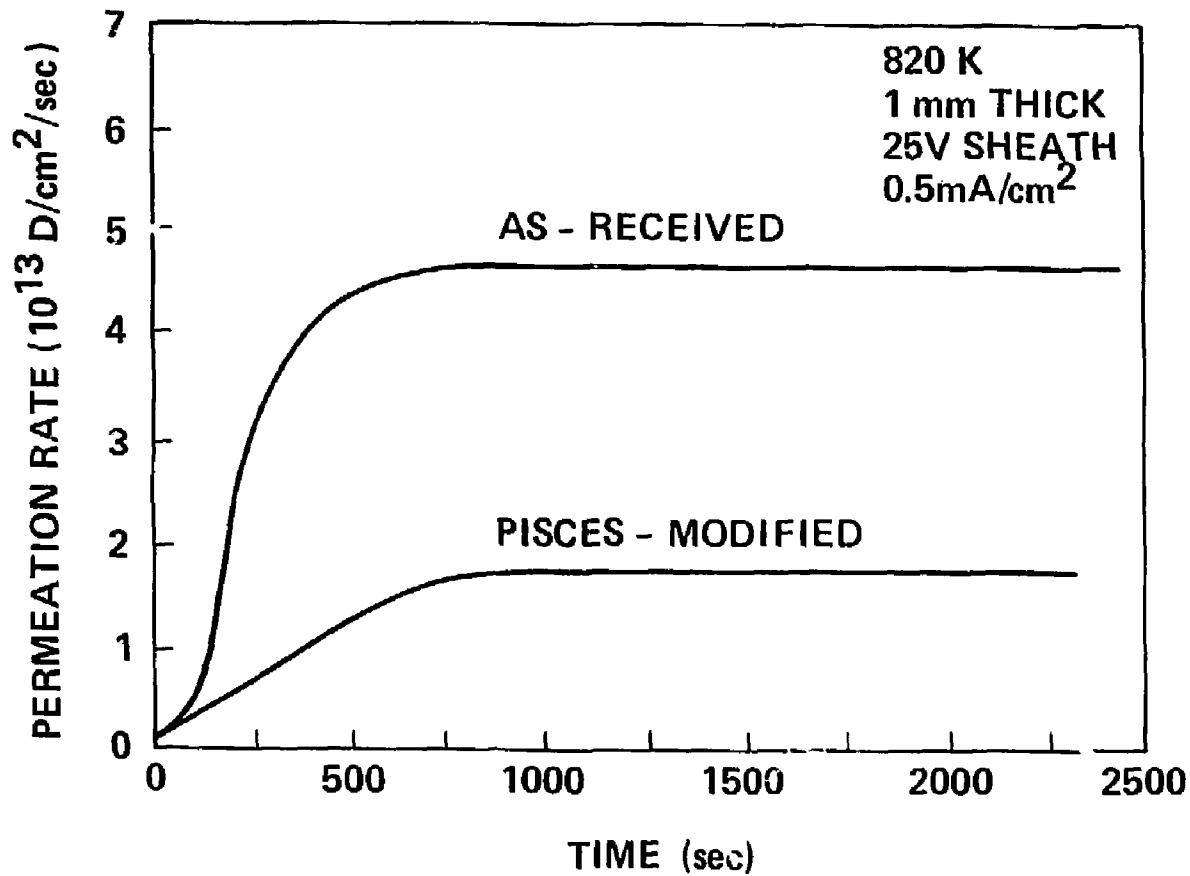


FIGURE 17